Interaction of Fixed Number of Photons with Retinal Rod Cells

Nam Mai Phan,[1,3] Mei Fun Cheng,[1] Dmitri A. Bessarab,[2] and Leonid A. Krivitsky[1,*]
[1]Data Storage Institute, Agency for Science Technology and Research (A-STAR), 117608, Singapore
[2]Institute of Medical Biology, Agency for Science Technology and Research (A-STAR), 138648, Singapore
[3]Department of Bioengineering, National University of Singapore, 117576, Singapore
(Received 18 December 2013; published 29 May 2014)

New tools and approaches of quantum optics offer a unique opportunity to generate light pulses carrying a precise number of photons. Accurate control over the light pulses helps to improve the characterization of photoinduced processes. Here, we study interaction of a specialized light source which provides flashes containing just one photon, with retinal rod cells of *Xenopus laevis* toads. We provide unambiguous proof of the single-photon sensitivity of rod cells without relying on the statistical modeling. We determine their quantum efficiencies without the use of any precalibrated detectors and obtain the value of $(29 \pm 4.7)\%$. Our approach provides the path for future studies and applications of quantum properties of light in phototransduction, vision, and photosynthesis.

DOI: 10.1103/PhysRevLett.112.213601 PACS numbers: 42.50.-p, 42.50.Dv, 42.66.Lc, 87.80.Jg

The ability to control light at a quantum level can be extremely useful in addressing biological problems. Studies of interaction of biological objects with nonclassical (quantum) light allow us to enhance the precision of biological measurements [1], fosters the development of more precise models of biological processes [2], and allows us to reveal the possible role of quantum effects in neurobiology [3,4] and perception [5,6].

Rod cells of the retina are natural photodetectors, and they are perfect candidates for studies of interaction of biological systems with quantum light. Rod cells convert incident light into electrical currents, which are then sent to the brain via the optics nerve. They are responsive at the discrete photon level, and highly sensitive techniques for the readout of their electrical response are readily available [7,8].

To date, only light sources with classical photon statistics (lasers, lamps, light emitting diodes, etc.) have been used in visual studies [9,10]. Quantum mechanics imposes a fundamental limit on the stability of such sources. The number of emitted photons is not fixed but rather follows a defined probability distribution, depending on the light source [11]. This leaves doubt about the exact number of photons used to stimulate the rod cell. The impact of unavoidable photon fluctuations becomes a crucial issue for the experiments conducted at the discrete photon level. Using the light source with a "fixed" number of photons would allow for a more precise and direct characterization of rod cells and facilitate the development of more accurate mathematical models for vision and phototransduction processes.

A number of methods for the reliable generation of light pulses with a fixed numbers of photons (Fock states) have been suggested [12]. It was theoretically proposed to use such pulses for the characterization of individual stages of the phototransduction [2], visual detection of quantum entanglement [3,4], and precise determination of the visual threshold [2,13].

In this Letter, we experimentally realize a "noise-free" single-photon light source and study its interaction with a biological object. Our experiment allows us to resolve several problems which cannot be addressed using light sources with classical photon statistics, including (1) demonstration of the single-photon sensitivity of rod cells without relying on statistical modeling, (2) precise determination of the parameters of rod cell single-photon responses without the interference from multiphoton detection events, and (3) accurate measurement of the quantum efficiency of rod cells without precalibrated devices.

We exploit spontaneous parametric down-conversion (SPDC) [14], which is known to be one of the most accessible and versatile approaches to the generation of single photons. In the SPDC, a photon of a laser pulse (pump), propagating in a nonlinear optical crystal, is converted with some probability ($\approx 10^{-6}$) into a pair of photons (signal and idler), obeying conservation of energy and momentum:

$$\omega_p = \omega_s + \omega_i; \qquad \vec{k}_p = \vec{k}_s + \vec{k}_i, \tag{1}$$

where $\omega_{p,s,i}$ and $\vec{k}_{p,s,i}$ are the frequencies and the wave vectors of the pump, signal, and idler photons, respectively. The conservation laws [Eq. (1)] guarantee that signal and idler photons have well defined frequencies and emission directions. In our experiment, we use a Q-switched Nd:YAG laser (Crystalaser, $\lambda_p = 266$ nm, pulse duration 30 ns, repetition rate 25 kHz) as a pump and a nonlinear 5 mm long β-barium borate (BBO) crystal. Signal and idler photons are emitted from the BBO in two directions, which form an angle of $\pm 3°$ to the direction of the pump; see Fig. 1. They have the same wavelengths $\lambda_s = \lambda_i = 532$ nm, which are chosen to maximize photon absorption by the rhodopsin photopigment in the cell [15,16].

Simultaneity in emission of signal and idler photons is used for the generation of single-photon pulses [17]. The

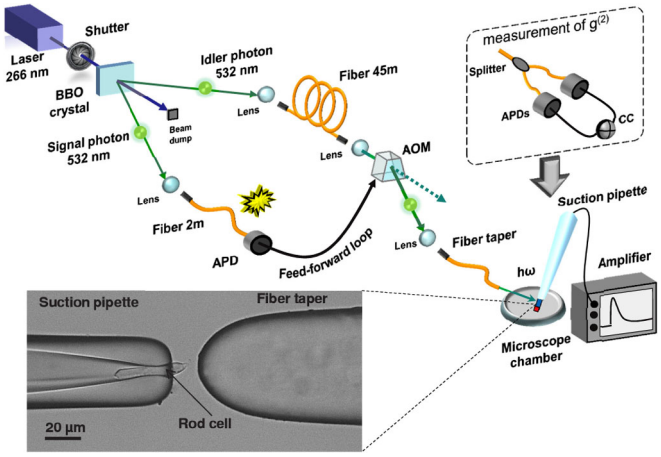

FIG. 1 (color online). Experimental setup. Photon pairs are produced via the spontaneous parametric down-conversion in the BBO crystal pumped by a UV laser. The signal photon is detected by the APD, and its output triggers an AOM. The idler photon is delayed by the fiber and then diverted by the AOM to a fiber taper pointing at a rod cell. Electrical currents of the rod cell are measured by the technique of the suction pipet. Single photons in the idler beam are characterized in a separate experiment by measuring $g^{(2)}$ using a 50/50 beam splitter, two APDs, and a CC; see the inset. A microscope (20×) image shows the rod cell in the suction pipet and the fiber taper in the recording configuration. Their positions are carefully aligned to ensure optimal light coupling.

signal photon is addressed to a single-photon avalanche photodiode (APD, Perkin-Elmer). The APD output is used as a trigger for an acousto-optical modulator (AOM, Gooch and Housego) in the idler beam; see Fig. 1. Once the signal photon is detected by the APD, the AOM is activated for a period of 100 ns, during which it diverts the idler photon to an optical fiber pointing at the rod cell. An idler photon is optically delayed by a 45 m long fiber to compensate for incurring delays. Details of the experiment synchronization are shown in Fig. S1 of the Supplemental Material [18]. If the APD does not detect a signal photon, the AOM remains inactive, and no light pulse is sent to the rod cell.

Ideally, each photocount of the APD in the signal beam heralds a single photon in the idler beam, which is directed to the rod cell. However, inefficiencies of optical elements in the idler beam lead to losses of some of the idler photons. We measured that the probability of a heralded idler photon to reach the rod cell is about 22%. The detailed analysis of optical losses is presented in the Supplemental Material [18].

Single-photon sources are conventionally characterized with the second order correlation function $g^{(2)}$

$$g^{(2)} = 1 + \frac{\mathrm{Var}N - \langle N\rangle}{\langle N\rangle^2}, \tag{2}$$

where $\langle N\rangle$ and $\mathrm{Var}N$ are the mean and the variance of the number of photons, respectively [20]. For Poissonian light sources, $g^{(2)} = 1$, while for an ideal single-photon source, $g^{(2)} = 0$. We measure $g^{(2)}$ of light in the idler beam in the independent experiment, using a 50/50 fiber beam splitter (Thorlabs) and two gated APDs (Perkin-Elmer). APD signals are addressed to a coincidence circuit (CC) with a time window of 120 ns (Phillips Scientific). Then, $g^{(2)} \propto N_c/(N_1N_2)$, where N_1 and N_2 are the numbers of APD photocounts and N_c is the number of photocount coincidences [20]. Our measurement yields $g^{(2)} = 0.08 \pm 0.06$. Thus, the probability of emission of more than one photon is about 12 times smaller, compared to the Poissonian light source with the same mean photon number. Details on the characterization of the single-photon source are described in Fig. S2 of the Supplemental Material [18]. The obtained value of $g^{(2)}$ compares favorably to the ones typically obtained with alternative single-photon sources [12].

Our light source also provides the possibility of measurement of the quantum efficiency of rod cells [21–23]. The quantum efficiency η characterizes the ability of rod cells to respond to the impinging light, and it is defined as

$$\eta \propto R/N_{\mathrm{APD}=1}, \tag{3}$$

where R is the number of rod cell responses and $N_{\mathrm{APD}=1}$ is the number of incident photons, which is proportional to the number of photocounts of the APD in the signal beam. In contrast to the conventional approach, it is a direct method of measurement, which does not require calibration of the photometer or optical standards, and it does not rely on the choice of any particular model of rod cell response.

Methods of cell preparation, electrophysiology recordings, and light coupling are similar to the ones we described previously [24,25]. Rod cells are obtained from dark-adapted adult male frogs (*Xenopus laevis*) [26]. Rod cells are loaded into a chamber of the inverted microscope placed in a light-tight Faraday cage. The microscope is equipped with an IR lamp and a CCD camera. The membrane current of the rod cell is measured with the electrophysiological technique of a suction pipet [7]. Pipets are pulled from a glass capillary, and their tips have openings in a range between 6 and 7 μm. The pipet is connected to the amplifier (Heka). Current waveforms are recorded with 100 Hz bandwidth, and, along with trigger pulses from the APD, they are saved to the computer for subsequent analysis.

The rod cell is held in a glass pipet, and a taper of an optical fiber (Nanonics) is positioned next to it; see Fig. 1. The light from the fiber propagates axially to the rod cell. Such an arrangement allows us to maximize photon absorption by the rod cell and mimics the way light travels in the eye [24]. The taper has a working distance of 22 μm and a spot size of 4 μm, chosen to match the size of the cell. The selection of the responsive rod cells and control of their functionality are described in detail in the Supplemental Material [18]. The experiments are conducted at room temperature (20° C). Results obtained from ten rod cells from ten different animals are presented.

Initially, a shutter blocks the pump beam, and the membrane current of the rod cell in the dark is recorded for 600 ms. The shutter is opened for 100 ms, and the current is recorded for 5 s. The waveform amplitude is calculated as a difference of the time-averaged membrane current at the peak of the response and at the baseline. The positions of time windows are defined individually for each rod cell by analyzing responses to pulses of an auxiliary laser. For each opening of the shutter, the APD may or may not produce a photocount. Waveforms accompanied by only a single APD photocount are used to analyze single-photon responses. Waveforms accompanied by zero photocounts are used to analyze the dark noise. Single-photon responses and the dark noise are measured concurrently.

The probability distribution of waveform amplitudes for the case when the APD heralds a single photon is shown in Fig. 2(a). It has an asymmetrical shape with the mean 0.07 pA and the variance 0.1 pA^2. A nonresponse peak, centered at 0 pA, corresponds to events when the rod cell fails to detect a photon or the photon was lost in the idler beam. A single-photon response peak, centered at 0.58 pA, corresponds to successful single-photon detection events. The histogram is fitted by a sum of two Gaussian peaks centered at 0 and 0.58 pA; both have a full width at half maximum (FWHM) of 0.5 pA. The fit yields a coefficient of determination $R^2 = 0.92$. The peaks partially overlap due to the experimental noise, which includes contributions from continuous and discrete components of the physiological noise of the rod cell [27,28] and the Johnson noise in the seal resistance.

Because of relatively small amplitudes of single-photon responses for *Xenopus laevis* toads [29,30], it was not possible to clearly separate them from the experimental noise. A more clear separation of the single-photon peak would be possible with *Bufo marinus* toads [9]. At the same time, the use of controllable single-photon stimulation guarantees that the observed asymmetry in the response histogram is caused by single-photon detection, even in a case in which signal photon signals are not clearly separated from the noise.

In Fig. 2(a), multiphoton responses are not observed, and their statistics follows the statistics of light with a single-photon precision [25]. Note that in order to minimize the contribution of multiphoton responses using light sources with classical photon statistics, it would be necessary to adjust its light strength in accordance with the quantum efficiency of each cell. The latter is not known in advance and may vary significantly due to biological factors. The use of our light source allows us to exclude bias in assessing single-photon responses for different cells, since it always provides strong suppression of the multiphoton component.

The distribution of dark noise amplitudes, shown in Fig. 2(b), has the mean 0 pA and variance 0.07 pA^2. It shows convolution of the physiological noise of the rod cell with the noise of the recording system [27,28]. The curve is fitted by a single Gaussian peak centered at 0 pA with FWHM = 0.59 pA ($R^2 = 0.97$).

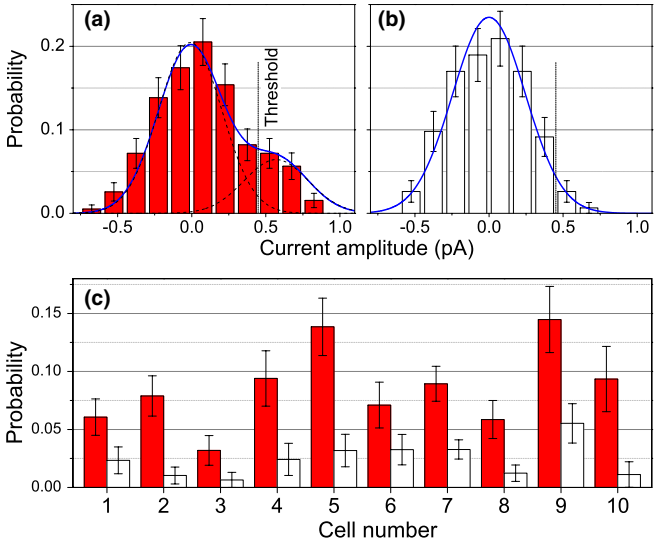

FIG. 2 (color online). (a) Probability distribution of amplitudes of rod cell responses when the APD in the signal beam heralds a single photon ($n = 195$) and (b) for the dark noise ($n = 157$). Solid lines are Gaussian fits. The vertical dashed lines indicate the criterion level for the categorization of single-photon responses. (c) Overall probability of the occurrence of single-photon responses, satisfying the criterion, when the APD heralds a single photon (red bars) and for the dark noise (white bars). The total number of experimental trials is 402 for cell 1, 435 for cell 2, 342 for cell 3, 273 for cell 4, 352 for cell 5, 353 for cell 6, 816 for cell 7, 449 for cell 8, 333 for cell 9, and 197 for cell 10. Error bars in (a)–(c) show ±s.d. Plots in (a) and (b) correspond to cell 5 in (c).

A criterion-based method is used to identify single-photon responses. Waveforms with amplitudes higher than the criterion level are categorized as single-photon responses, and those that are lower than the criterion level are categorized as nonresponses. Based on the measurement of the noise of the amplifier—see Fig. S3 of the Supplemental Material [18]—the criterion level is set at 0.45 pA.

We apply the amplitude threshold criterion (> 0.45 pA) and sum all the probabilities for responses satisfying the criterion. The probability of the occurrence of single-photon responses is higher when the APD heralds a single photon, compared to the dark noise; see Fig. 2(c). The hypothesis is tested with Welch's unpaired t test [31]. The one-tailed P value is 0.028 for cell 1, 0.00015 for cell 2, 0.039 for cell 3, 0.006 for cell 4, 0.0001 for cell 5, 0.053 for cell 6, 0.0005 for cell 7, 0.005 for cell 8, 0.003 for cell 9, and 0.006 for cell 10. Therefore, the responsiveness of the cells to stimuli produced by the single-photon source is justified. Thus, we provide a model-independent proof of the single-photon sensitivity of rod cells, which was never attempted before. The cell-to-cell variations are mainly attributed to the intrinsic differences of cells to respond to single photons because they originated from different animals and were obtained from different parts of the retina.

The averaged waveforms of single-photon responses and nonresponses for cell 5 are shown in Figs. 3(a) and 3(b). It

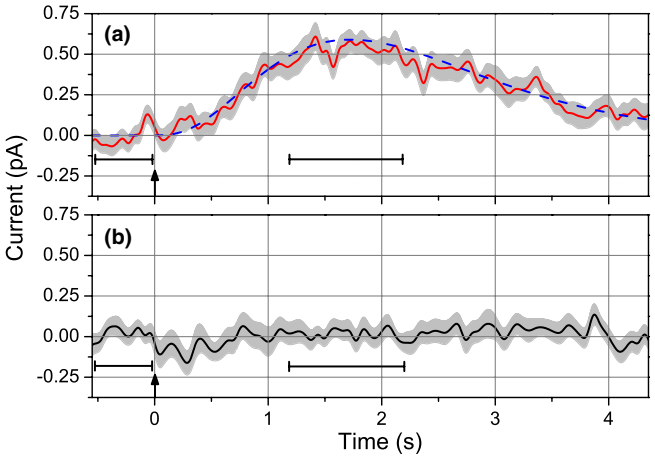

FIG. 3 (color online). (a) Average waveform of the cell single-photon responses (solid red line) and (b) of nonresponses (bandwidth 20 Hz, $n = 27$). The dashed blue line in (a) is the theoretical curve. The arrow indicates the moment of opening of the shutter in the pump beam. Horizontal bars show time windows for the calculation of waveform amplitudes. Grey shaded regions in (a) and (b) show ±s.e.m. Plots in (a) and (b) correspond to cell 5 in Fig. 2(c).

is fitted with the impulse response of the Poisson filter $i(t) = A_0[t/t_0 \exp(1 - t/t_0)]^{(m-1)}$ with the amplitude $A_0 = 0.58$ pA, number of stages $m = 4$, and time to peak $t_0 = 1.75$ s [32]. The waveform parameters for all the studied cells are shown in Fig. S4 of the Supplemental Material [18]. The responses have the amplitude (0.59 ± 0.01) pA, time to peak (1.8 ± 0.2) s, and duration at the full width at half maximum (2.2 ± 0.2) s (mean ± s.e.m., $n = 10$). The mean values are close to the ones observed in experiments with conventional light sources and rod cells from the same species [29,30]. However, due to the use of the controllable single-photon source, the dependence of the observed fluctuations of response parameters on the number of incident photons is excluded. This opens the opportunity to directly assess the intrinsic noise of the phototransduction process in rod cells, which is hindered by the presence of multiphoton events in experiments using light sources with classical statistics [2,33].

The quantum efficiencies of rod cells are calculated from data in Fig. 2(c) by taking into account optical losses in the idler channel and the rod cell dark noise, according to Eq. (S2) of the Supplemental Material [18]. The result yields $\eta = (29 \pm 4.7)\%$ (mean ± s.e.m., $n = 10$). In earlier experiments, the rod cell of a *Bufo marinus* toad was illuminated by a transverse stripe of light [9]. The probability of photon absorption was measured as 11.9%, and the efficiency of the response to the absorbed photon was measured as 50%, which together result in $\eta = 6\%$. Our results are consistently (≈5 times) higher than this, since we use an axial geometry of photon delivery and the proper single-photon source, which excludes the presence of multiphoton events. It is interesting that our result is close to the estimate of Ref. [10] for human rod cells, obtained from behavioral experiments. Note that in SPDC, the wavelengths of signal and idler photons can be tuned in a very broad range [14]. Hence, it is possible to use this approach for measurement of the spectral dependence of the quantum efficiency. Moreover, since the results obtained by the method do not depend on the used equipment, its implementation would ensure the integrity and credibility of the relevant biological data emerging from different labs.

In conclusion, we performed an experiment, where we send light pulses from a true single-photon source, based on the SPDC, to the rod cell via an optical fiber, and measure the rod cell responses. We provide a direct and unambiguous proof of the single-photon sensitivity of rod cells, characterize their single-photon responses without any interference from multiphoton events, and measure their quantum efficiencies without using any precalibrated devices. Our approach is universal and direct, as it is not based on any particular statistical model of the cell response and it does not involve any indirect assumptions.

The approach can be directly extended to study responses of the whole visual system to controllable multiphoton stimulation; see the Supplemental Material [18] for details. Such an experiment will allow precise determination of the visual threshold [2,13] and address a fundamental question about the manifestation of quantum effects in neurobiology [3,4].

The presented approach opens a way for exploiting quantum light in studies of other photoinduced processes, such as photosynthesis. The ultimate control over photon statistics could lead to new clues about the manifestation of quantum coherence in such processes [34–36]. From an engineering standpoint, it could help to define the properties required for a single-photon detector, mimicking natural detection, with retinal rod cells forming the basis.

We thank Nigel Sim, Alex Tok, and Mike Jones for their help at various stages of the project. We thank Gleb Maslennikov, Vadim Volkov, John Dowling, and Trevor Lamb for valuable comments. The work is done with the financial support of A-STAR Joint Council Office Grant No. 1231AEG025.

*Leonid_Krivitskiy@dsi.a-star.edu.sg

[1] M. A. Taylor, J. Janousek, V. Daria, J. Knittel, B. Hage, H.-A. Bachor, and W. P. Bowen, Nat. Photonics **7**, 229 (2013).
[2] M. C. Teich, P. R. Prucnal, G. Vannucci, M. E. Breton, and W. J. McGill, Biol. Cybern. **44**, 157 (1982).
[3] P. Sekatski, N. Brunner, C. Branciard, N. Gisin, and C. Simon, Phys. Rev. Lett. **103**, 113601 (2009).
[4] E. Pomarico, B. Sanguinetti, P. Sekatski, H. Zbinden, and N. Gisin, New J. Phys. **13**, 063031 (2011).
[5] F. H. Thaheld, BioSystems **71**, 305 (2003).
[6] Ch. Koch and K. Hepp, Nature (London) **440**, 611 (2006).
[7] D. A. Baylor, T. D. Lamb, and K. W. Yau, J. Physiol. **288**, 589 (1979).

[8] R. D. Bodoia and P. B. Detwiler, J. Physiol. **367**, 183 (1985).
[9] D. A. Baylor, T. D. Lamb, and K. W. Yau, J. Physiol. **288**, 613 (1979).
[10] F. Rieke and D. A. Baylor, Rev. Mod. Phys. **70**, 1027 (1998).
[11] R. Loudon, *The Quantum Theory of Light* (Oxford University Press, New York, 2000).
[12] M. D. Eisaman, J. Fan, A. Migdall, and S. V. Polyakov, Rev. Sci. Instrum. **82**, 071101 (2011).
[13] R. Holmes, B. G. Christensen, W. Street, R. F. Wang, and P. G. Kwiat, in *Proceedings of Quantum Electronics and Laser Science Conference, San Jose, California, United States, 2012* (Optical Society of America, Washington, DC, United States, 2012).
[14] D. N. Klyshko, *Photons and Nonlinear Optics* (Gordon and Breach, New York, 1988), p. 285.
[15] F. I. Harosi, J. Gen. Physiol. **66**, 357 (1975).
[16] A. G. Palacios, R. Srivastava, and T. H. Goldsmith, Visual neuroscience **15**, 319 (1998).
[17] J. G. Rarity, P. R. Tapster, and E. Jakeman, Opt. Commun. **62**, 201 (1987).
[18] See Supplemental Material at http://link.aps.org/supplemental/10.1103/PhysRevLett.112.213601 for details of the synchronization of the experiment, characterization of the single-photon source, measurement of the noise of the amplifier, choice of functional rod cells, calculation of quantum efficiency, and multiphoton responses, which includes Ref. [19].
[19] M. Avenhaus, K. Laiho, M. V. Chekhova, and Ch. Silberhorn, Phys. Rev. Lett. **104**, 063602 (2010).
[20] D. N. Klyshko, *Physical Foundations of Quantum Electronics* (World Scientific, Singapore, 2011), p. 318.
[21] D. C. Burnham and D. L. Weinberg, Phys. Rev. Lett. **25**, 84 (1970).
[22] A. A. Malygin, A. N. Penin, and A. V. Sergienko, Sov. Phys. JETP Lett. **33**, 477 (1981).
[23] A. Migdall, Phys. Today **52**, 1, 41 (1999).
[24] N. Sim, D. Bessarab, C. M. Jones, and L. A. Krivitsky, Biomed. Opt. Express **2**, 2926 (2011).
[25] N. Sim, M. F. Cheng, D. Bessarab, C. M. Jones, and L. A. Krivitsky, Phys. Rev. Lett. **109**, 113601 (2012).
[26] All procedures with animals are carried under Institutional Animal Care and Use Committee (IACUC) regulations.
[27] D. A. Baylor, G. Matthews, and K. W. Yau, J. Physiol. **309**, 591 (1980).
[28] F. Rieke and D. A. Baylor, Neuron **26**, 181 (2000).
[29] V. Kefalov, Y. Fu, N. Marsh-Armstrong, and K.-W. Yau, Nature (London) **425**, 526 (2003).
[30] E. Solessio *et al.*, J. Gen. Physiol. **124**, 569 (2004).
[31] B. L. Welch, Biometrika **34**, 28 (1947).
[32] D. A. Baylor, A. L. Hodgkin, and T. D. Lamb, J. Physiol. **242**, 685 (1974).
[33] M. C. Teich, P. R. Prucnal, G. Vannucci, M. E. Breton, and W. J. McGill, J. Opt. Soc. Am. **72**, 419 (1982).
[34] G. S. Engel, T. R. Calhoun, E. L. Read, T.-K. Ahn, T. Mančal, Y.-C. Cheng, R. E. Blankenship, and G. R. Fleming, Nature (London) **446**, 782 (2007).
[35] E. Collini, C. Y. Wong, K. E. Wilk, P. M. G. Curmi, P. Brumer, and G. D. Scholes, Nature (London) **463**, 644 (2010).
[36] P. Brumer and M. Shapiro, Proc. Natl. Acad. Sci. U.S.A. **109**, 19575 (2012).